THE JOURNAL OF PHYSICAL CHEMISTRY LETTERS
A JOURNAL OF THE AMERICAN CHEMICAL SOCIETY

pubs.acs.org/JPCL

Letter

Reactions of H_2, HD, and D_2 with H_2^+, HD^+, and D_2^+: Product-Channel Branching Ratios and Simple Models

Frédéric Merkt,* Katharina Höveler, and Johannes Deiglmayr

Cite This: *J. Phys. Chem. Lett.* 2022, 13, 864−871

Read Online

ACCESS | Metrics & More | Article Recommendations

ABSTRACT: We present measurements of the product-channel branching ratios of the reactions (i) $HD^+ + HD$ forming $H_2D^+ + D$ (38.1(30)%) and $HD_2^+ + H$ (61.9(30)%), (ii) $HD^+ + D_2$ forming $HD_2^+ + D$ (61.4(35)%) and $D_3^+ + H$ (38.6(35)%), and (iii) $D_2^+ + HD$ forming $HD_2^+ + D$ (60.5(20)%) and $D_3^+ + H$ (39.5(20)%) at collision energies E_{coll} near zero, i.e., below $k_B \times 1$ K. These branching ratios are compared with branching ratios predicted using three simple models: a combinatorial model (M1), a model (M2) describing the reactions as H-, H^+-, D-, and D^+-transfer processes, and a statistical model (M3) that relates the reaction rate coefficients to the translational and rovibrational state densities of the $H_nD_{3-n}^+ + H/D$ (n = 0, 1, 2 or 3) product channels. The experimental data are incompatible with the predictions of models M1 and M2 and reveal that the branching ratios exhibit clear correlations with the product state densities.

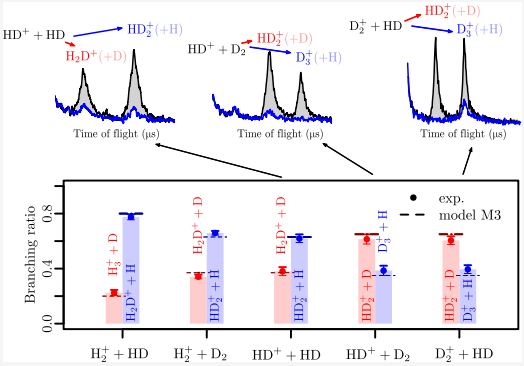

The reactions between molecular hydrogen (H_2, HD, and D_2) and molecular hydrogen ions (H_2^+, HD^+, and D_2^+) are reactions involving only four nuclei and three electrons and are used to test theories of chemical reactivity (e.g., refs 1−5). They play an important role in astrophysics[6−9] and plasma physics[10] and have been the object of numerous experimental studies of the collision- and internal-energy dependences of the cross sections, angular distributions, and branching ratios to the different product channels (e.g., refs 11−23). Studies of the reactions involving partially and fully deuterated species provide important information on the reaction mechanisms.[4,11−14,18,24−26] Table 1 summarizes the possible reactions at low temperatures or low collision energies, where the contributions of charge-transfer reactions (e.g., $HD^+ + D_2 \rightarrow HD + D_2^+$) and collision-induced dissociation (e.g., $H_2^+ + D_2 \rightarrow H^+ + H + D_2$) play a negligible role (Figure 1 in ref 18 and ref 4). These reactions can be formally described in terms of H-, H^+-, D-, or D^+-transfer processes, as listed in the column labeled "M2" in Table 1. For each pair of competing reactions (e.g., reactions (2a,b), (3a,b), etc.), the product-ion ratios directly reflect the ratios of the respective rate coefficients. Typical values for these rate coefficients used to model the chemical composition of cold, low-density plasmas from ref 10 are listed in the last column of Table 1. The remaining columns of Table 1 provide values of the 0 K reaction energies for these reactions ($\Delta_i U(0\ K)$) and for the corresponding charge-transfer reactions ($\Delta_{i,CT} U(0\ K)$), which we have derived from literature values of the dissociation and ionization energies of H_2,[27,28] HD,[29] and D_2,[30] the dissociation energy of H_2^+,[31] the ionization energies of H[32] and D,[33] the dissociation energy of H_3^+,[34] and the zero-point energies of H_3^+, H_2D^+, HD_2^+, and D_3^+.[35]

The product-ion ratios can be used to test hypotheses concerning the reaction mechanisms; they can also be used to test classical, semiclassical, and full quantum-mechanical scattering calculations, including nonadiabatic effects, of the reaction rates as a function of the temperature, the collision energy, and the rovibrational states of the reactants. For instance, Douglass et al. concluded from the identical product ratios of reactions (6a,b) and (8a,b) that rapid charge equilibration must occur during the product formation and that the reactions take place adiabatically on the ground-state potential-energy surface at low energies.[13] Krenos et al.[12] and Pollard et al.[18] found that the reactions must follow a direct mechanism without the formation of a long-lived four-nuclei−three-electron intermediate complex. Several early studies reported that the ratios depend on the collision energy or the temperature.[13,36]

Recently, we have developed a merged-beam method to study ion−molecule reactions at very low collision energies,[20,37] down to below $k_B \times 1$ K. (k_B is Boltzmann's constant.) This method is described in detail in ref 37. It relies

Received: October 14, 2021
Accepted: November 30, 2021
Published: January 19, 2022

Table 1. Reactions Involving the Neutral Molecules H_2, HD, and D_2 and the Ions H_2^+, HD^+, and D_2^+ and their 0 K Reaction Energies $\Delta_i U(0\ K)$

reaction index i	reactants	products	$\Delta_i U(0\ K)/(hc)$ (cm^{-1})	M2[a]	$\Delta_{i,CT} U(0\ K)/(hc)$ (cm^{-1})[b]	k ($m^3\ s^{-1}$)[c]
1	$H_2^+ + H_2$	$H_3^+ + H$	−13 967(2)	H^+, H	0	2.0×10^{-9}
2a	$H_2^+ + HD$	$H_3^+ + D$	−13 560(2)	H	150.9947(6)	$0.25 \times 2 \times 10^{-9}$
2b		$H_2D^+ + H$	−13 920(15)	H^+, D		$0.75 \times 2 \times 10^{-9}$
3a	$H_2^+ + D_2$	$H_2D^+ + D$	−13 578(15)	D	327.90264(6)	$0.50 \times 3.2 \times 10^{-9}$
3b		$HD_2^+ + H$	−13 994(15)	H^+		$0.50 \times 3.2 \times 10^{-9}$
4a	$HD^+ + H_2$	$H_3^+ + D$	−13 711(2)	H^+	−150.9947(6)	$0.25 \times 2.0 \times 10^{-9}$
4b		$H_2D^+ + H$	−14 071(15)	D^+, H		$0.75 \times 2.0 \times 10^{-9}$
5a	$HD^+ + HD$	$H_2D^+ + D$	−13 784(15)	H^+, H	0	0.80×10^{-9}
5b		$HD_2^+ + H$	−14 200(15)	D^+, D		1.00×10^{-9}
6a	$HD^+ + D_2$	$HD_2^+ + D$	−13 858(15)	H^+, D	176.9079(6)	$0.67 \times 2.0 \times 10^{-9}$
6b		$D_3^+ + H$	−14 307(15)	D^+		$0.33 \times 2.0 \times 10^{-9}$
7a	$D_2^+ + H_2$	$H_2D^+ + D$	−13 905(15)	D^+	−327.90264(6)	$0.5 \times 3.2 \times 10^{-9}$
7b		$HD_2^+ + H$	−14 323(15)	H		$0.5 \times 3.2 \times 10^{-9}$
8a	$D_2^+ + HD$	$HD_2^+ + D$	−14 035(15)	D^+, H	−176.9079(6)	$0.67 \times 1.8 \times 10^{-9}$
8b		$D_3^+ + H$	−14 484(15)	D		$0.33 \times 1.8 \times 10^{-9}$
9	$D_2^+ + D_2$	$D_3^+ + D$	−14 141(2)	D^+, D	0	1.6×10^{-9}

[a]Describes the reaction in terms of H, H^+, D, or D^+ transfer. [b]0 K reaction energies of the corresponding charge-transfer reactions. [c]Rate constants of the reactions specified by the second and third columns used to model low-temperature, low-density hydrogen plasmas.[10]

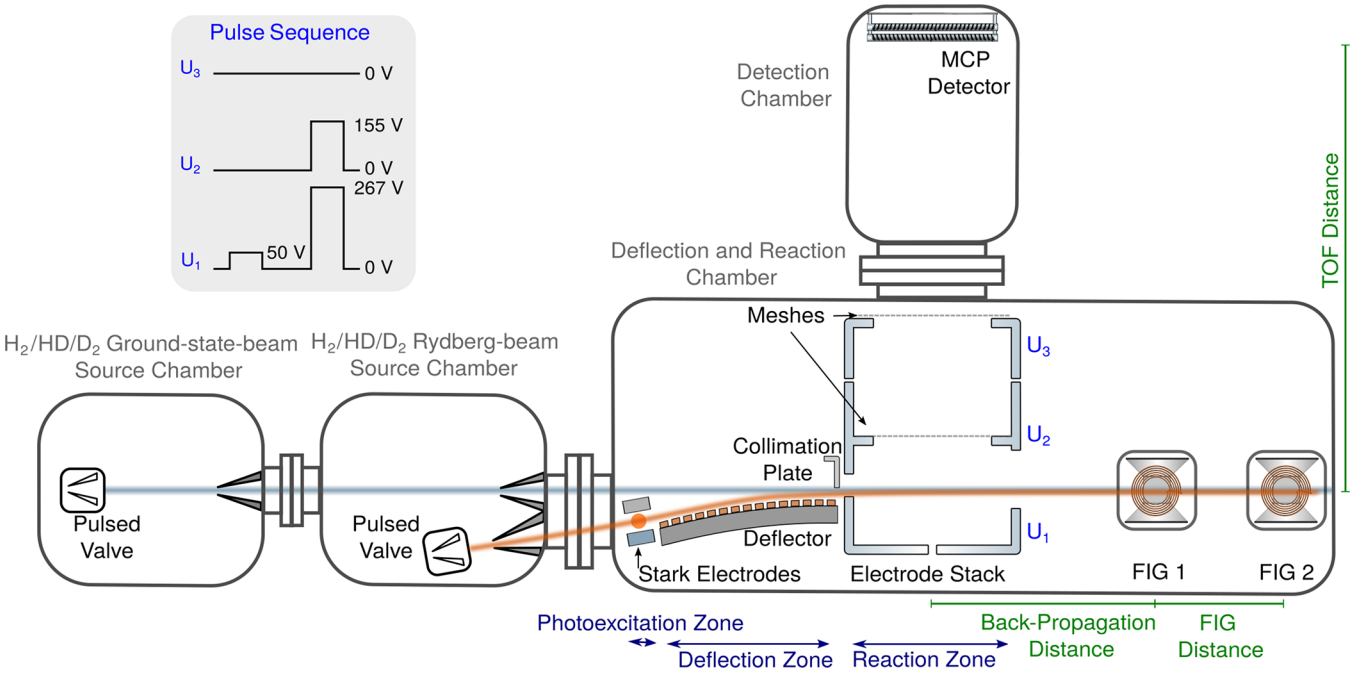

Figure 1. Schematic representation of the experimental setup with the gas-source chambers, the supersonic beams (orange and pale-blue lines), the photoexcitation region and the Rydberg−Stark deflector, the reaction zone located within the electrode stack used to extract the ions, the MCP detector used to monitor the product ions, and the fast-ionization gauges (FIG 1 and FIG 2) used to characterize the ground-state beam. See the text for details.

on the observation of the ion−molecule reaction within the orbit of a highly excited Rydberg electron which neither participates in the reaction nor significantly influences it but prevents the reactant ions from being accelerated by stray electric fields in the reaction volume. Consequently, the branching ratios of several of the reactions listed in Table 1 can now be measured for the first time near zero collision energies. This letter presents new results on the branching ratios of reactions (5a,b), (6a,b), and (8a,b) and complements results on reactions (2a,b) and (3a,b) obtained recently.[22,23] Our method cannot be used to determine the branching ratios of reactions (4a,b) and (7a,b) because it relies on time-of-flight mass spectrometry to detect the product ions, and the mass resolution is not sufficient to distinguish reactant and product ions of the same mass number (e.g., HD^+ from H_3^+ in reaction (4a)). The branching ratios obtained for reactions (2a,b), (3a,b), (5a,b), (6a,b), and (8a,b) are, however, sufficient to draw conclusions on the factors that determine their values. The purpose of this letter is to present our new measurements of branching ratios and discuss them in comparison to the predictions of simple models.

The experimental procedure and the experimental setup used to measure branching ratios in the reactions of molecular hydrogen (H_2, HD, and D_2) and the hydrogen molecular ions

https://doi.org/10.1021/acs.jpclett.1c03374
J. Phys. Chem. Lett. 2022, 13, 864−871

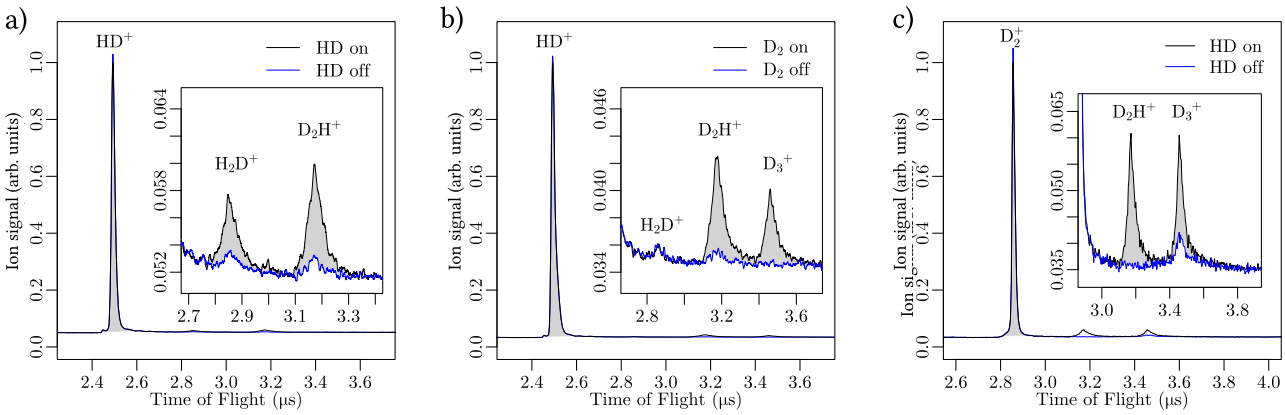

Figure 2. Time-of-flight mass spectra of the ions present in the reaction zone at the end of a 5-μs-long reaction-observation window for (a) the HD^+ + HD reaction forming H_2D^+ and HD_2^+, (b) the HD^+ + D_2 reaction forming HD_2^+ and D_3^+, and (c) the D_2^+ + HD reaction forming HD_2^+ and D_3^+. The insets display the spectra in the region of the product-ion signals on an enlarged scale. The black and blue lines represent the signals measured with the ground-state beam turned on and off, respectively, and the areas shaded in gray correspond to the product-ion signals. See the text for details.

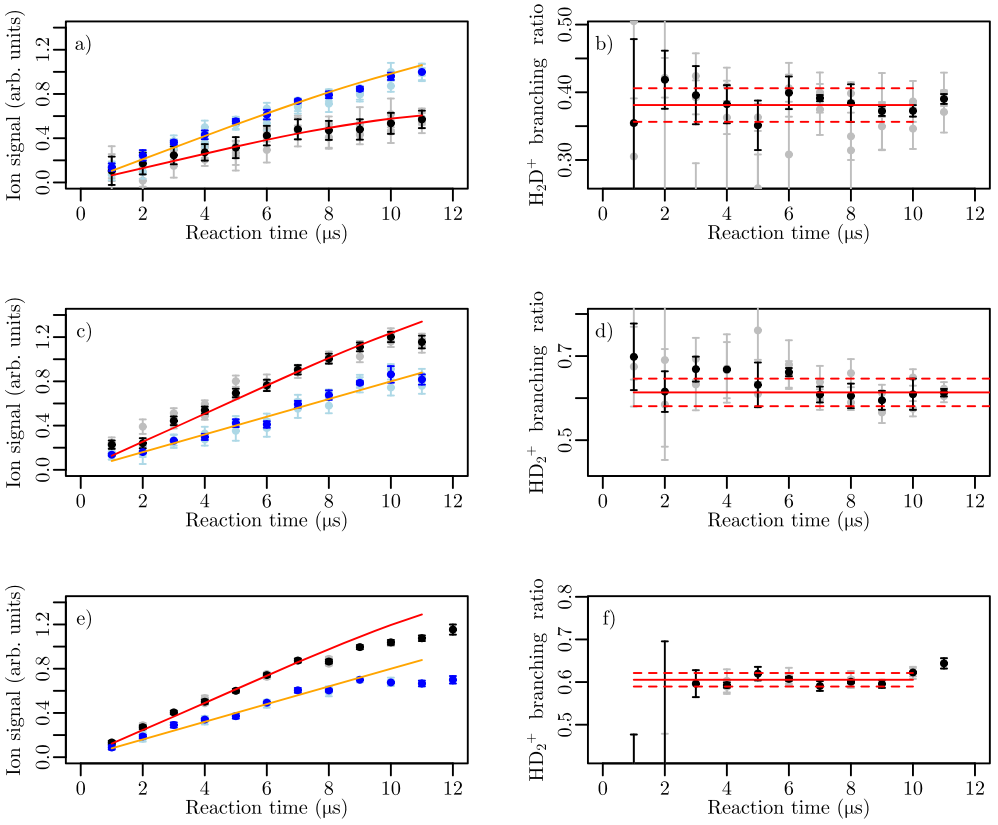

Figure 3. Determination of the product branching ratios $\frac{[H_2D^+]}{[H_2D^+]+[HD_2^+]}$ of the HD^+ + HD reaction (panels (a) and (b)), $\frac{[HD_2^+]}{[HD_2^+]+[D_3^+]}$ of the HD^+ + D_2 reaction (panels (c) and (d)), and $\frac{[HD_2^+]}{[HD_2^+]+[D_3^+]}$ of the D_2^+ + HD reaction (panels (e) and (f)). Panels (a), (c), and (e) display the normalized, background-corrected ion signals as a function of the duration τ of the reaction-observation window (called the reaction time). The dots with error bars (1σ) and the solid lines represent the measured signals and the scaled calculated detection functions, respectively. Panels (b), (d), and (f) show the branching ratios as dots with error bars. The solid and dashed red horizontal lines indicate the mean values and the weighted standard deviations, respectively. The results of independent measurements are depicted in dark and pale colors.

(H_2^+, HD^+, and D_2^+) have been described in detail in refs 22 and 23. Only the main aspects of the measurements are summarized here. A schematic view of the experimental setup is presented in Figure 1. A supersonic beam of ground-state HD or D_2 molecules (referred to as the ground-state beam) generated by a short-pulse cryogenic home-built valve delivering 20-μs-long pulses at a repetition rate of 25 Hz is doubly skimmed and propagates in a straight line through the reaction zone. Its spatial, temporal, and velocity distributions are determined using two fast ionization gauges (FIG 1 and FIG 2 in the figure) located at accurately known positions along the propagation axis beyond the reaction zone. The HD

https://doi.org/10.1021/acs.jpclett.1c03374
J. Phys. Chem. Lett. 2022, 13, 864−871

molecules in the HD ground-state beam are almost exclusively in their absolute, $J = 0$ ground rotational level. The D_2 molecules in the D_2 supersonic beam are also in their absolute rotational ground states (i.e., $J = 0$ for ortho D_2 (two-thirds of the molecules) and $J = 1$ for para D_2 (one-third of the molecules).

A second supersonic beam of either HD or D_2 is produced by another similar home-built valve. Its propagation axis initially makes a 10° angle with the propagation axis of the first beam. After passing through a skimmer and two sets of baffles, the molecules are excited to long-lived Rydberg−Stark states of principal quantum number $n = 27$ having an ion core in the $X^+\,^2\Sigma_g^+(v^+ = 0, N^+ = 0)$ rovibronic ground state. A triply resonant three-photon excitation sequence is used via selected rovibrational levels of the intermediate B $^1\Sigma_u^+$ and I $^1\Pi_g^+$ electronic states, as described in ref 38.

A curved surface-electrode Rydberg−Stark deflector and decelerator[39] is used to merge the beam of Rydberg molecules with the ground-state beam. Reactions between the ground-state and the Rydberg molecules are monitored for a predefined and adjustable temporal reaction-observation window of duration τ, at the end of which the product ions are accelerated toward a microchannel-plate (MCP) detector by applying a large electric potential across the reaction zone. The reaction-observation window is initialized by applying a weak electric field that removes all ions present in the reaction zone and is terminated by the ion-extraction pulse just mentioned (inset of Figure 1). The product ions arrive at distinct times at the MCP detector, and their integrated signals are used to determine the branching ratios of the two product channels, as explained in more detail in the next section.

The results presented in this article were obtained by setting the velocities of the ground-state beam and the Rydberg-molecule beam so that the collision energy was near 0 (i.e., below $k_B \times 1$ K (details in ref 22)) with a collision-energy bandwidth of less than $k_B \times 400$ mK.

The solid black lines in panels (a)−(c) of Figure 2 show typical time-of-flight mass spectra obtained after a reaction-observation time of $\tau = 5$ μs for the $HD^+ + HD$ reaction forming H_2D^+ and HD_2^+, the $HD^+ + D_2$ reaction forming HD_2^+ and D_3^+, and the $D_2^+ + HD$ reaction forming HD_2^+ and D_3^+, respectively. In each of these mass spectra, the two possible triatomic ionic products are observed as distinct peaks, as clearly seen in the insets. To obtain the branching ratios for the two product channels for each of the reaction systems, the ground-state beam is turned on and off in alternate experimental cycles to determine and then subtract the background ion signals (blue lines in Figure 2) generated by reactions of the Rydberg molecules with H_2, HD, or D_2 molecules in the background gas of the vacuum chamber. The relative product-ion yields are determined by integrating the background-corrected ion signals over the corresponding time-of-flight ranges and correspond to the areas shaded in gray in Figure 2. They are further normalized, on a shot-to-shot basis, by dividing the integrated signals by the relative densities of (i) the molecules in the ground-state beam monitored at the fast ionization gauges and (ii) the Rydberg molecules measured by pulsed-field ionization.

To determine the branching ratios of the competing reaction channels, measurements such as those presented in Figure 2 are repeated for different τ values. The procedure is illustrated in Figure 3 for the three reaction systems [(5a,b), (6a,b), and (8a,b)]. This figure shows in panels (a), (c), and (e) the normalized and background-corrected integrated signals $I(H_nD_{3-n}^+)$ of the two triatomic-ion products originating from the two competing reaction channels as blue and black dots with error bars (i.e., $I(H_2D^+)$ (black) and $I(HD_2^+)$ (blue) in panel (a) and $I(HD_2^+)$ (black) and $I(D_3^+)$ (blue) in panels (c) and (e)). For $\tau \leq 5$ μs, the product-ion signals grow linearly with τ, reflecting the fact that the density of the ground-state molecules is much higher than the density of the Rydberg molecules. Typically less than 1% of the Rydberg molecules undergo a reaction in the reaction zone so that the ion yields are directly proportional to the rate coefficients. For $\tau \geq 5$ μs, the product-ion signals do not grow as fast because some of the ions emitted with the highest kinetic energy may leave the detection volume. Lighter product ions are on average emitted with a higher velocity than the heavier ones and leave the detection volume earlier, which needs to be considered when determining the branching ratios. The correction is done through a full numerical simulation of the particle trajectories, as explained in detail in ref 22. The solid orange and red lines in panels (a), (c), and (e) correspond to the expected normalized signals predicted by taking the detection losses evaluated in numerical particle-trajectory simulations into account based on the product-kinetic-energy distributions determined in separate experiments (refs 22 and 23) as well as in earlier work.[13,18] The good agreement between measured and simulated signals up to about $\tau = 10$ μs enables us to correct for the detection losses. Panels (b), (d), and (f) of Figure 3 depict the branching ratios

$$\eta_{(5a,b)} = \frac{I(H_2D^+)}{I(H_2D^+) + I(HD_2^+)}$$
$$\eta_{(6a,b)} = \frac{I(HD_2^+)}{I(HD_2^+) + I(D_3^+)}$$
$$\eta_{(8a,b)} = \frac{I(HD_2^+)}{I(HD_2^+) + I(D_3^+)} \quad (1)$$

determined from the respective corrected product-ion signals. For two competing reactions generating ion products i and j, the branching ratio $\eta_i = I_i/(I_i + I_j)$ is related to the ratio $r_{ij} = I_i/I_j$ of product-ion signals I_i and I_j through

$$\eta_i = \left(1 + \frac{1}{r_{ij}}\right)^{-1} \quad (2)$$

The solid and dashed red lines in panels (b), (d), and (f) represent the mean values of the branching ratios and their standard deviations, respectively. These branching ratios and the branching ratios obtained in similar experiments for reaction pairs (2a,b) and (3a,b)[22,23] are listed in the column labeled η_{exp} in Table 2.

The branching ratios for reactions (2a,b), (3a,b), (5a,b), (6a,b), and (8a,b) listed in Table 2 can be used for comparison with the predictions of theoretical models. In the following text, three simple models are discussed which are inspired by considerations made in the discussion of earlier investigations.[4,11−14,18,24−26] The first model, M1, is the simplest one and considers only the probability of randomly drawing the neutral-atom product (H or D) from the four atoms involved in the reactions, assuming equal probabilities of drawing each atom. This model appears to be at the origin of the prefactors of some of the rate coefficients used to model the composition of cold plasmas of H_2 and D_2 (e.g., the values reported in ref 10 for reactions (2a,b), (3a,b), (4a,b), and (7a,b) which are listed

https://doi.org/10.1021/acs.jpclett.1c03374
J. Phys. Chem. Lett. 2022, 13, 864−871

Table 2. Comparison of the Branching Ratios of the Ion−Molecule Reactions Involving the Neutral Molecules H_2, HD, and D_2 and the Ions H_2^+, HD^+, and D_2^+ Calculated with Model M1 (η_{M1}) and Model M3 (η_{M3}) with the Branching Ratios η_{exp} Measured at Collision Energies E_{coll} near Zero (i.e., below $k_B \times 1$ K)[a]

reaction	reactants	products	η_{exp}	η_{M1}	η_{M3}
2a	$H_2^+ + HD$	$H_3^+ + D$	0.225(20)[b]	0.25	0.20
2b		$H_2D^+ + H$	0.775(20)[b]	0.75	0.80
3a	$H_2^+ + D_2$	$H_2D^+ + D$	0.341(15)[c]	0.50	0.37
3b		$HD_2^+ + H$	0.659(15)[c]	0.50	0.63
4a	$HD^+ + H_2$	$H_3^+ + D$		0.25	0.20
4b		$H_2D^+ + H$		0.75	0.80
5a	$HD^+ + HD$	$H_2D^+ + D$	0.381(30)[d]	0.50	0.37
5b		$HD_2^+ + H$	0.619(30)[d]	0.50	0.63
6a	$HD^+ + D_2$	$HD_2^+ + D$	0.614(35)[d]	0.75	0.65
6b		$D_3^+ + H$	0.386(35)[d]	0.25	0.35
7a	$D_2^+ + H_2$	$H_2D^+ + D$		0.50	0.37
7b		$HD_2^+ + H$		0.50	0.43
8a	$D_2^+ + HD$	$HD_2^+ + D$	0.605(30)[d]	0.75	0.65
8b		$D_3^+ + H$	0.395(30)[d]	0.25	0.35

[a]The numbers in parentheses represent the statistical uncertainties (1σ). [b]From ref 23. [c]From ref 24. [d]This work.

in the last column of Table 1). The η values predicted by M1 are listed in the column labeled η_{M1} in Table 2. For instance, the branching ratios of reactions $H_2^+ + HD \rightarrow H_3^+ + D$ and $H_2^+ + HD \rightarrow H_2D^+ + H$ (2a,b) are predicted to be 0.25 and 0.75, respectively. Whereas this model seems to work well for these two particular reactions, it fails in all other cases for which branching ratios were measured at low collision energies.

The second model, M2, follows a more "chemical" approach and classifies the different reactions in terms of H/D-atom- or H^+/D^+-ion-transfer processes based on the reaction formulas and the assumption that a given atom- or ion-transfer process takes place at the same rate regardless of whether the other nuclei in the reaction system are protons or deuterons. In this model, the branching ratios can be expressed as a function of four rate constants: k_{H^+}, k_H, k_{D^+}, and k_D. For instance, the product-ion ratio and the branching ratio for the reaction pair (6a,b) are (see the column labeled "M2" in Table 1 and eq 2)

$$\frac{I(HD_2^+)}{I(D_3^+)} = \frac{k_{H^+} + k_D}{k_{D^+}} \text{ and}$$

$$\eta_{HD_2^+} = \frac{I(HD_2^+)}{I(HD_2^+) + I(D_3^+)} = \frac{k_{H^+} + k_D}{k_{H^+} + k_D + k_{D^+}} \quad (3)$$

Similar equations can be formulated for the other four reaction pairs (2a,b), (3a,b), (5a,b), and (8a,b). Three of these five equations can be used with the corresponding measured branching ratios to express k_{H^+}, k_{D^+}, and k_D in terms of k_H, and the model assumptions can be checked for internal consistency with the two remaining measured branching ratios. For instance, one obtains

$$k_{H^+} = 2.27k_H,\ k_D = 1.17k_H,\ \text{and}\ k_{D^+} = 4.14k_H \quad (4)$$

from the product-ion ratios measured for reactions (2a,b), (3a,b), and (6a,b). With these values, the product-ion ratio $I(HD_2^+)/I(D_3^+)$ from the reaction pair (8a,b) is predicted to be (see column "M2" in Table 1)

$$\frac{I(HD_2^+)}{I(D_3^+)} = \frac{k_{D^+} + k_H}{k_D} = 4.37 \quad (5)$$

which is incompatible with the value of 1.53 obtained experimentally. This model thus misrepresents the actual processes, and the H, D, H^+, and D^+ transfers are either not independent processes or the rate constants of the individual transfers depend on the nature of the remaining three nuclei. Introducing transfer rate coefficients that would depend on the other nuclei would increase the numbers of rate coefficients from 4 to 12, making the problem undetermined even if branching ratios were available from experiments for all reaction pairs listed in Tables 1 and 2. In this context, it may be relevant to note that previous studies have suggested that charge equilibration by charge transfer during the collision prevents the distinction between H^+ and H transfer[12,18] and that no obvious connection could be made between the endothermicity or exothermicity of the charge-transfer reactions (see the $\Delta_{i,CT}U(0\ K)$ values in Table 1) and the deviations of the experimental branching ratios from the predictions of models M1 and M2.

Nevertheless, useful insights result. First, one sees from the branching ratio obtained for the reaction pair (5a,b) that the combination of H^+ and H transfer is slower than the combination of D^+ and D transfer, which is surprising at first sight given the lighter masses. Second, the reaction pairs leading to identical products (i.e., (6a,b) and (8a,b) and to a lesser extent also (3a,b) and (5a,b)) have very similar branching ratios, although M2 expresses these ratios with different sets of rate constants. The equivalence of the branching ratios of the reaction pairs (6a,b) and (8a,b) had been emphasized earlier by Douglass et al.,[13] who concluded that rapid charge transfer during product formation makes atom and ion transfers indistinguishable. Both observations indicate that the branching ratios are product-specific and not reactant-specific. Moreover, the only factor that could favor transfers of D^+/D over H^+/H in reactions (5a,b) is an increased product state density resulting from the smaller rotational and vibrational constants in HD_2^+ (D^+/D transfer) compared to those in H_2D^+ (H^+/H transfer).

This analysis suggests, as the third model, a statistical model (M3) in which the rate coefficients are proportional to the corresponding translational- and rovibrational-state densities of the products, i.e., the number of translational and rovibrational quantum states per unit energy available at the energy with which the products are formed. M3 thus expresses the product-ion ratios for each pair of reactions in Table 1 as ratios of the corresponding translational- and rovibrational-state densities of the products. Anicich and Futrell[1] have advocated a related treatment of the formation of H_3^+ from H_2^+ and vibrationally excited H_2 but disregarding the effects of the rotational-state densities, which are found to be significant in the present case (see below).

The implementation of M3 is facilitated by the following facts:

- (i) The reactants are in their ground states. Neglecting the $J = 1$ rotational ground-state energy of ortho H_2 and para D_2, their internal energies can be taken to be zero.
- (ii) All reactions listed in Table 1 have approximately the same 0 K reaction energies, $\Delta_i U(0\ K)$ (i.e., $-hc \times 14\,000 \pm 500\ cm^{-1}$, -1735 ± 60 meV, or $-k_B \times 20\,200(750)$ K).

https://doi.org/10.1021/acs.jpclett.1c03374
J. Phys. Chem. Lett. 2022, 13, 864−871

- (iii) The product kinetic energies are similar in all cases and are about one-third of $\Delta_i U(0\ \mathrm{K})$. The internal rovibrational energies of the triatomic product ions are thus about two-thirds of $\Delta_i U(0\ \mathrm{K})$ (i.e., $hc \times 9300 \pm 500\ \mathrm{cm}^{-1}$, 1150 meV, or $k_B \times 13\ 400$ K), which is so large that the rotational- and vibrational-state densities can be expressed with reasonable accuracy in the high-energy approximation.

Using this approximation, the state density ρ_i of the products of reaction i can be expressed as

$$\rho_i \propto \sqrt{\mu_i} \times \frac{1}{\sigma_i \sqrt{\tilde{A}\tilde{B}\tilde{C}}} \times \frac{1}{\tilde{\nu}_1\tilde{\nu}_2\tilde{\nu}_3} \tag{6}$$

where the three successive terms correspond to the contributions of the relative translational motion of the products (i.e., of a one-dimensional translational motion), of the rotational motion of the triatomic product ion, and of its vibrational motion, respectively. The ratio $r_{ij} = I_i/I_j$ of the product-ion yields of the two competing reactions (i and j) of each pair is thus

$$r_{ij} = \frac{I_i}{I_j} = \frac{\sqrt{\mu_i}}{\sqrt{\mu_j}} \frac{\sigma_j}{\sigma_i} \frac{\sqrt{\tilde{A}_j\tilde{B}_j\tilde{C}_j}}{\sqrt{\tilde{A}_i\tilde{B}_i\tilde{C}_i}} \frac{\tilde{\nu}_{1j}\tilde{\nu}_{2j}\tilde{\nu}_{3j}}{\tilde{\nu}_{1i}\tilde{\nu}_{2i}\tilde{\nu}_{3i}} \tag{7}$$

In eqs 6 and 7, μ_n ($n = i, j$) is the reduced mass of the products of reaction n, σ_n is the symmetry number of the triatomic product ion of reaction n (i.e., 2 for H_2D^+ and HD_2^+ and 6 for H_3^+ and D_3^+), $\tilde{\nu}_{kn}$ represents the harmonic wave numbers of the three vibrational modes ($k = 1-3$), and $\tilde{A}_n$, $\tilde{B}_n$, and $\tilde{C}_n$ are the rotational constants. The values of σ_n reflect that the equivalent nuclei are indistinguishable. Consequently, the ratio σ_j/σ_i in eq 7 corresponds to the predictions of M1.

The purpose of this treatment is not to achieve a high numerical accuracy but to identify some of the factors determining the branching ratios. Consequently, we take for $\tilde{\nu}_{kn}$ and $\tilde{A}_n$, $\tilde{B}_n$, and $\tilde{C}_n$ the ground-state fundamental vibrational wave numbers and rotational constants, respectively, which are precisely known from experiments and *ab initio* calculations. With the full set of values reported for these quantities by Miller and Tennyson,[40] we obtain the branching ratios listed in the column "η_{M3}" in Table 2.

A comparison of these η_{M3} values with the branching ratios obtained experimentally for the reaction pairs (2a,b), (3a,b), (5a,b), (6a,b), and (8a,b) leads to the following conclusions. The overall trends are well reproduced, with maximal deviations for the reaction pair (8a,b), for which M3 predicts a value of 0.65 instead of 0.605(20), and the reaction pair (6a,b), for which M3 predicts a value of 0.65 instead of 0.614(35)%. For the reaction pairs (2a,b), (3a,b), and (5a,b), the agreement is almost within the experimental uncertainties and certainly also within the uncertainties inherent in the model assumptions and approximations. This statement applies, in particular, to reactions (3a) and (3b), which are formally pure D and H^+ transfers, respectively.

Whereas the high-energy approximation is entirely justified for the rotational-state densities, it is expected to be accurate only to about 20% for the vibrational-state densities and to be least accurate for the lightest triatomic ion products. However, a significant part of the errors in the state densities cancels out in the ratios (eq 7). Model M3 does not require an equipartition of the reaction energy among the different degrees of freedom. For it to be valid, it suffices that (i) the products are formed over a broad range of states, (ii) the average energy in each degree of freedom of the products is sufficient for the high-energy approximation, and (iii) for each pair of reactions, the average energy in a given degree of freedom is similar for both sets of products. For instance, the same results are obtained for 20, 30, and 50% partitions of the reaction energy among the translational, rotational, and vibrational degrees of freedom, respectively, as for an equipartition. Available data[13,18,22,23] suggest that the kinetic energies released for the two reactions of each pair differ by less than 10%, and quasiclassical trajectory calculations indicate product-state distributions that differ from equipartition.[2]

Analyzing the different contributions to the product ratios from eq 7 indicates that the dominant contribution stems from the symmetry numbers, which disfavor by a factor of 3 the formation of $H_3^+ + D$ compared to $H_2D^+ + H$ in reaction pairs (2a,b) and (4a,b) and the formation of $D_3^+ + H$ compared to $HD_2^+ + D$ in reaction pairs (6a,b) and (8a,b). The contributions of rotational- (without symmetry number) and vibrational-state densities both favor the formation of the heavier triatomic product ion by factors ranging from 1.2 to 1.5. The contributions to the ratios from the translational-state densities are the smallest and never exceed a factor of 1.25.

In this letter, we have presented the results of measurements at very low collision energies, below $k_B \times 1$ K, of all branching ratios of the reactions of H_2, HD, and D_2 with H_2^+, HD^+, and D_2^+ that can be determined by time-of-flight mass spectrometry in our experiments. We have tried to rationalize the experimental observations with three very simple models: a purely combinatorial model (M1), a model classifying the reactions as proton, deuteron, H-atom, and D-atom transfers assuming that the rates are independent of the nature of nontransferred atoms (M2), and a statistical model assuming that the reaction rates are proportional to the product state densities (M3). Whereas the first two models proved inadequate, the results of the analysis with statistical model M3 satisfactorily reproduced the main trends observed experimentally. This agreement strongly suggests (but does not prove) that the product state densities are an important factor determining the branching ratios at very low collision energies. The state densities, however, cannot be the sole factor because if they were then the experimental branching ratios of reaction pairs (3a,b) and (5a,b) would have been the same but they differ by ~15%. Moreover, the branching ratios for several of the reaction pairs discussed here are known to strongly depend on the collision energy. (See refs 11 and 24 for early experimental observations and ref 4 for a recent theoretical description of this phenomenon.) Our measured branching ratios and their corresponding simple modeling with M3 are for reactants in their ground states and are limited to the low-collision-energy regime.

Statistical theories and models are commonly used to interpret the results of elementary reactions, and their validity ranges are well established. (See refs 41−43 and also ref 44 for applications to ion−molecule capture reactions involving H_2^+.) A common justification for the treatment of reaction rates with statistical theories is the formation of a long-lived intermediate complex along the reaction path. Calculations of the potential energy surfaces of the reaction of H_2^+ and H_2 reveal that the reaction is downhill without a local well corresponding to a van der Waals complex of the type $H_2^+-H_2$ in the entrance channel (e.g., Figure 1 in ref 45 and Figures 2 and 4 in ref 4). A weakly bound van der Waals complex of the type H_3^+-H exists in the

https://doi.org/10.1021/acs.jpclett.1c03374
J. Phys. Chem. Lett. 2022, 13, 864−871

exit channel[4,45] but is not expected to be relevant for the dynamics of the strongly exothermic reactions discussed here.

An alternative justification for a statistical treatment for a strongly exothermic, barrier-free reaction would be that the distribution of product states is simply dominated by the number of product channels and is independent of the details of the dynamics. For the reactions between H_2 and H_2^+ and their deuterated isotopomers, the motions in the full seven-dimensional phase space are very different for the reactants and products so that a broad distribution of the reaction energy over the product degrees of freedom is not surprising. In this case, eq 7 would result if the restrictions on the product states imposed by the conservation of total angular momentum, parity, and nuclear symmetry[46−48] are not too severe or too different for the two reactions of each reaction pair in Tables 1 and 2. For the range of collision energies probed in our experiments, partial waves with l up to at least 5 significantly contribute to the capture rates (e.g., Figure 5 in ref 5), which reduces the effects of the restrictions imposed by the conservation of parity and total angular momentum. The conservation of nuclear-spin symmetry is likely to play a more significant role and may contribute to the observed differences in the branching ratios of reactions (3a,b) and (5a,b).

In the future, it would be important to assess the limits of model M3 more rigorously both experimentally and theoretically. The determination of the branching ratios of reaction pairs (4a,b) and (7a,b), which could not be determined using the time-of-flight mass-spectrometric method used in the present investigation, would also be desirable for comparison with the model predictions.

AUTHOR INFORMATION

Corresponding Author

Frédéric Merkt − *Laboratorium für Physikalische Chemie, ETH Zürich, 8093 Zürich, Switzerland;* orcid.org/0000-0002-4897-2234; Email: frederic.merkt@phys.chem.ethz.ch

Authors

Katharina Höveler − *Laboratorium für Physikalische Chemie, ETH Zürich, 8093 Zürich, Switzerland*

Johannes Deiglmayr − *Laboratorium für Physikalische Chemie, ETH Zürich, 8093 Zürich, Switzerland;* Present Address: Department of Physics, University of Leipzig, DE-04109 Leipzig, Germany

Complete contact information is available at: https://pubs.acs.org/10.1021/acs.jpclett.1c03374

Notes

The authors declare no competing financial interest.

ACKNOWLEDGMENTS

We thank Dr. Urs Hollenstein and Dr. Raphael Hahn for experimental assistance, Hansjürg Schmutz and Josef A. Agner for technical support, and Prof. Martin Quack (ETH Zurich), Prof. Jeremy Richardson (ETH Zurich), Prof. Octavio Roncero (Madrid), and Prof. Jonathan Tennyson (University College London) for useful discussions and insightful comments on a previous version of this letter. This work is supported financially by the Swiss National Science Foundation (grant no. 200020B-200478) and by the European Research Council through the ERC Advanced Grant (grant no. 743121) under the European Unions Horizon 2020 Research and Innovation Program.

REFERENCES

(1) Anicich, V. G.; Futrell, J. H. A computer study of the formation of H_3^+ and its vibrational deactivation using a statistical model. *Int. J. Mass Spectrom. Ion Processes* **1984**, *55*, 189−215.

(2) Eaker, C. W.; Schatz, G. C. A quasiclassical trajectory study of the $H_2^+ + H_2 \rightarrow H_3^+ + H$ reaction. *J. Phys. Chem.* **1985**, *89*, 2612−2620.

(3) Stine, J. R.; Muckerman, J. T. Critical evaluation of classical trajectory surface-hopping methods as applied to the $H_2^+ + H_2$ system. *J. Phys. Chem.* **1987**, *91*, 459−466.

(4) Sanz-Sanz, C.; Aguado, A.; Roncero, O.; Naumkin, F. Non-adiabatic couplings and dynamics in proton transfer reactions of H_n^+ systems: Application to $H_2 + H_2^+ \rightarrow H + H_3^+$ collisions. *J. Chem. Phys.* **2015**, *143*, 234303.

(5) Dashevskaya, E. I.; Litvin, I.; Nikitin, E. E.; Troe, J. Relocking of intrinsic angular momenta in collisions of diatoms with ions: Capture of H_2 (j = 0, 1) by H_2^+. *J. Chem. Phys.* **2016**, *145*, 244315.

(6) Herbst, E.; Klemperer, W. The formation and depletion of molecules in dense interstellar clouds. *Astrophys. J.* **1973**, *185*, 505.

(7) Herbst, E. Chemistry in the interstellar medium. *Annu. Rev. Phys. Chem.* **1995**, *46*, 27−53.

(8) Gay, C. D.; Stancil, P. C.; Lepp, S.; Dalgarno, A. The highly deuterated chemistry of the early universe. *Astrophys. J.* **2011**, *737*, 44.

(9) Oka, T. Interstellar H_3^+. *Chem. Rev.* **2013**, *113*, 8738−8761.

(10) Jiménez-Redondo, M.; Carrasco, E.; Herrero, V. J.; Tanarro, I. Isotopic exchange processes in cold plasmas of H_2/D_2 mixtures. *Phys. Chem. Chem. Phys.* **2011**, *13*, 9655−9666.

(11) Futrell, J. H.; Abramson, F. P. Effect of translational energy on ion−molecule reaction rates. *Adv. Chem. Ser.* **1967**, *58*, 107−130.

(12) Krenos, J. R.; Lehmann, K. K.; Tully, J. C.; Hierl, P. M.; Smith, G. P. Crossed-beam study of the reactions of H_2^+ with D_2 and D_2^+ with H_2. *Chem. Phys.* **1976**, *16*, 109−116.

(13) Douglass, C. H.; McClure, D. J.; Gentry, W. R. The dynamics of the reaction $H_2^+ + H_2 \rightarrow H_3^+ + H$ with isotopic variations. *J. Chem. Phys.* **1977**, *67*, 4931−4940.

(14) Hierl, P. M.; Herman, Z. Crossed-beam study of the reaction $H_2^+ + D_2 \rightarrow D_2H^+ + H$. *Chem. Phys.* **1980**, *50*, 249−254.

(15) Anderson, S. L.; Houle, F. A.; Gerlich, D.; Lee, Y. T. The effect of vibration and translational energy on the reaction dynamics of the $H_2^+ + H_2$ system. *J. Chem. Phys.* **1981**, *75*, 2153−2162.

(16) Shao, J. D.; Ng, C. Y. A vibrational state-selected study of the reaction $H_2^+(v_0') + H_2(v'' = 0) \rightarrow H_3^+ + H$ using the tandem photoionization mass spectrometry and radio frequency ion guide methods. *J. Chem. Phys.* **1986**, *84*, 4317−4326.

(17) Guyon, P. M.; Baer, T.; Cole, S. K.; Govers, T. R. The charge transfer and collision-induced dissociation cross sections of state selected H_2^+ and D_2^+ ions. *Chem. Phys.* **1988**, *119*, 145−158.

(18) Pollard, J. E.; Johnson, L. K.; Lichtin, D. A.; Cohen, R. B. State-selected reactive scattering. I. $H_2^+ + H_2 \rightarrow H_3^+ + H$. *J. Chem. Phys.* **1991**, *95*, 4877−4893.

(19) Glenewinkel-Meyer, T.; Gerlich, D. Single and merged beam studies of the reaction $H_2^+(v = 0, 1; j = 0, 4) + H_2 \rightarrow H_3^+ + H$. *Isr. J. Chem.* **1997**, *37*, 343−352.

(20) Allmendinger, P.; Deiglmayr, J.; Höveler, K.; Schullian, O.; Merkt, F. Observation of enhanced rate coefficients in the $H_2^+ + H_2 \rightarrow H_3^+ + H$ reaction at low collision energies. *J. Chem. Phys.* **2016**, *145*, 244316.

(21) Savić, I.; Schlemmer, S.; Gerlich, D. Formation of H_3^+ in collisions of H_2^+ with H_2 studied in a guided ion beam instrument. *ChemPhysChem* **2020**, *21*, 1429−1435.

(22) Höveler, K.; Deiglmayr, J.; Agner, J. A.; Schmutz, H.; Merkt, F. The $H_2^+ + HD$ reaction at low collision energies: H_3^+/H_2D^+ branching ratio and product-kinetic-energy distributions. *Phys. Chem. Chem. Phys.* **2021**, *23*, 2676−2685.

(23) Höveler, K.; Deiglmayr, J.; Merkt, F. Deviation of the rate of the $H_2^+ + D_2$ reaction from Langevin behaviour below 1 K, branching

ratios for the HD_2^+ + H and H_2D^+ + D product channels, and product-kinetic-energy distributions. *Mol. Phys.* **2021**, *119*, e1954708.
(24) Bowers, M. T.; Elleman, D. D.; King, J. Analysis of the ion−molecule reactions in gaseous H_2, D_2, and HD by ion cyclotron resonance techniques. *J. Chem. Phys.* **1969**, *50*, 4787−4804.
(25) Lees, A. B.; Rol, P. K. Merging beams study of the $H_2^+(H_2,H)H_3^+$, $H_2^+(D_2,H)HD_2^+$, and $D_2^+(H_2,H)HD_2^+$ reaction mechanisms. *J. Chem. Phys.* **1974**, *61*, 4444−4449.
(26) Picconatto, C. A.; Gellene, G. I. A classical trajectory study of possible symmetry restrictions in the H_2^+/H_2 proton/atom transfer reaction. *J. Phys. Chem.* **1993**, *97*, 13629−13636.
(27) Hölsch, N.; Beyer, M.; Salumbides, E. J.; Eikema, K. S. E.; Ubachs, W.; Jungen, Ch.; Merkt, F. Benchmarking theory with an improved measurement of the ionization and dissociation energies of H_2. *Phys. Rev. Lett.* **2019**, *122*, 103002.
(28) Beyer, M.; Hölsch, N.; Hussels, J.; Cheng, C.-F.; Salumbides, E. J.; Eikema, K. S. E.; Ubachs, W.; Jungen, Ch.; Merkt, F. Determination of the interval between the ground states of para- and ortho-H_2. *Phys. Rev. Lett.* **2019**, *123*, 163002.
(29) Sprecher, D.; Liu, J.; Jungen, Ch.; Ubachs, W.; Merkt, F. The ionization and dissociation energies of HD. *J. Chem. Phys.* **2010**, *133*, 111102.
(30) Liu, J.; Sprecher, D.; Jungen, Ch.; Ubachs, W.; Merkt, F. Determination of the ionization and dissociation energies of the deuterium molecule (D_2). *J. Chem. Phys.* **2010**, *132*, 154301.
(31) Korobov, V. I.; Hilico, L.; Karr, J.-P. Fundamental transitions and ionization energies of the hydrogen molecular ions with few ppt uncertainty. *Phys. Rev. Lett.* **2017**, *118*, 233001.
(32) Tiesinga, E.; Mohr, P. J.; Newell, D. B.; Taylor, B. N. CODATA recommended values of the fundamental physical constants: 2018. *Rev. Mod. Phys.* **2021**, *93*, 025010.
(33) Yerokhin, V. A.; Pachucki, K.; Patkóš, V. Theory of the Lamb shift in hydrogen and light hydrogen-like ions. *Ann. Phys. (Berlin, Ger.)* **2019**, *531*, 1800324.
(34) Mizus, I. I.; Polyansky, O. L.; McKemmish, L. K.; Tennyson, J.; Alijah, A.; Zobov, N. F. A global potential energy surface for H_3^+. *Mol. Phys.* **2019**, *117*, 1663−1672.
(35) Ramanlal, J.; Polyansky, O. L.; Tennyson, J. Zero point energy of H_3^+ and its deuterated isotopomers. *Astron. Astrophys.* **2003**, *406*, 383−384.
(36) Huntress, W. T.; Elleman, D. D.; Bowers, M. T. Dependence of the rates on ion kinetic energy for the reactions $D_2^+ + D_2$ and $HD^+ +$ HD. *J. Chem. Phys.* **1971**, *55*, 5413−5414.
(37) Allmendinger, P.; Deiglmayr, J.; Schullian, O.; Höveler, K.; Agner, J. A.; Schmutz, H.; Merkt, F. New method to study ion−molecule reactions at low temperatures and application to the $H_2^+ + H_2 \rightarrow H_3^+ +$ H reaction. *ChemPhysChem* **2016**, *17*, 3596−3608.
(38) Seiler, Ch.; Hogan, S. D.; Merkt, F. Trapping cold molecular hydrogen. *Phys. Chem. Chem. Phys.* **2011**, *13*, 19000−19012.
(39) Allmendinger, P.; Deiglmayr, J.; Agner, J. A.; Schmutz, H.; Merkt, F. Surface-electrode decelerator and deflector for Rydberg atoms and molecules. *Phys. Rev. A: At., Mol., Opt. Phys.* **2014**, *90*, 043403.
(40) Miller, S.; Tennyson, J. First principles calculation of the molecular constants of H_3^+, H_2D^+, D_2H^+, and D_3^+. *J. Mol. Spectrosc.* **1987**, *126*, 183−192.
(41) Quack, M.; Troe, J. Information, memory and statistical theories of elementary chemical reactions. *Ber. Bunsenges. Phys. Chem.* **1976**, *80*, 1140−1149.
(42) Quack, M. Statistical models for product energy distributions in bimolecular reactions with metastable intermediates. *Chem. Phys.* **1980**, *51*, 353−367.
(43) Quack, M.; Troe, J. Statistical methods in scattering. *Theoretical Chemistry: Adances and perspectives* **1981**, *6B*, 199−276.
(44) Dashevskaya, E. I.; Litvin, I.; Nikitin, E. E.; Troe, J. Rates of complex formation in collisions of rotationally excited homonuclear diatoms with ions at very low temperatures: Application to hydrogen isotopes and hydrogen-containing ions. *J. Chem. Phys.* **2005**, *122*, 184311.
(45) Stine, J. R.; Muckerman, J. T. Charge exchange and chemical reaction in the $H_2^+ + H_2$ system. I. Characterization of the potential energy surfaces and nonadiabatic regions. *J. Chem. Phys.* **1978**, *68*, 185.
(46) Quack, M. Detailed symmetry selection rules for reactive collisions. *Mol. Phys.* **1977**, *34*, 477−504.
(47) Quack, M. On the densities and numbers of rovibronic states of a given symmetry species: Rigid and nonrigid molecules, transition states, and scattering channels. *J. Chem. Phys.* **1985**, *82*, 3277−3283.
(48) Uy, D.; Cordonnier, M.; Oka, T. Observation of ortho-para H_3^+ selection rules in plasma chemistry. *Phys. Rev. Lett.* **1997**, *78*, 3844.

https://doi.org/10.1021/acs.jpclett.1c03374
J. Phys. Chem. Lett. 2022, 13, 864−871